



Cite this: *Polym. Chem.*, 2025, **16**, 4136

## Degradable polyacetals and polyacetal/ polycyclooctene Co-polymers from a novel dioxepin

Andrew Mazza, Brian H. Morrow,  Judith A. Harrison  and Julia Pribyl  \*

Self-amplified degradable polyacetals and degradable polyacetal/polycyclooctene co-polymers were prepared *via* ring-opening metathesis polymerization (ROMP) of a newly-reported 3-bromopropyl-functionalized dioxepin monomer. Despite the relatively low ring-strain energy (RSE) of the monomer (calculated to be 4.34 kcal mol<sup>-1</sup>) compared to other small cyclic olefins, homopolymerization produced 3-bromopropyl-functionalized polyacetals up to  $M_n = 9.15$  kg mol<sup>-1</sup>. Acid catalyzed degradation experiments monitored by nuclear magnetic resonance (NMR) spectroscopy revealed the degradation to be self-amplifying in nature, since each instance of acetal hydrolysis released an equivalent of HBr. Co-polymerization of *cis*-cyclooctene and the 3-bromopropyl-functionalized dioxepin resulted in successful co-polymerization. The co-polymers degraded into small polycyclooctene fragments in acidic media, which was evidence the co-polymerization was successful, and the degradable acetal linkages were incorporated in multiple places along the co-polymer backbone.

Received 15th May 2025,  
Accepted 18th August 2025

DOI: 10.1039/d5py00484e

rsc.li/polymers

### Introduction

Degradability is an important property to consider when designing polymers for biological applications<sup>1–3</sup> or for imparting recyclability<sup>4</sup> or circularity<sup>5–8</sup> into synthetic materials. Incorporation of hydrolytically labile ester linkages into polymer backbones *via* ring-opening polymerization (ROP) is the classic strategy to incorporate hydrolytically-sensitive functionality while leveraging the inherent benefits of chain-growth chemistry.<sup>9–12</sup> Recently, more exotic degradable polymers have been prepared using olefin metathesis chemistry<sup>13,14</sup> including polyoxazinanes,<sup>15</sup> polyacetals,<sup>16–21</sup> poly(sulfonate esters),<sup>19</sup> alternating polyacetals/polyketals,<sup>22</sup> poly(*ortho* esters),<sup>23</sup> poly(silyl ethers),<sup>24</sup> poly(enol ethers),<sup>25–29</sup> polyphosphonates,<sup>30</sup> polypyrophosphates,<sup>31</sup> poly(disulfides),<sup>32,33</sup> polycarbonates,<sup>34</sup> and polyphosphoramidates.<sup>35</sup>

Of the mentioned examples, acetals are an elegant choice of degradable moiety. Acetals are perhaps best known as an effective protecting group for carbonyl-containing organic compounds; they can be quantitatively deprotected (degraded) under mildly acidic conditions and are robust to most other conditions. Polyacetals exhibit moderate to fast degradation kinetics compared to other degradable polymers prepared with metathesis chemistry.<sup>14</sup> When thinking about the fate of degradable polymers, mild, acid-triggered degradation is

attractive because pH gradients are common in environmental and biological systems.<sup>36</sup>

The work reported herein began by designing a newly-reported dioxepin monomer inspired by the 3-iodopropyl acetal incorporated into  $\alpha,\omega$ -dienes for acyclic diene metathesis (ADMET) polymerization reported by the Zimmerman group.<sup>21</sup> Homopolymerization of the dioxepin *via* ring-opening metathesis polymerization (ROMP) was studied, and the resulting homopolymers were found to exhibit self-amplifying degradation characteristics in acidic media. Statistical co-polymers synthesized from the dioxepin and *cis*-cyclooctene revealed that the dioxepin was incorporated into polyethylene precursors under the right polymerization conditions, and this platform may prove useful in incorporating degradability into polyolefins.

### Results and discussion

Synthesis of a cyclic olefin containing a 3-bromopropyl acetal group was carried out in one step (shown in Scheme 1) according to a modified procedure from the literature.<sup>37</sup> Briefly, 3-bromopropionaldehyde dimethyl acetal (**1**), *cis*-2-butene-1,4-diol (**2**), and *p*-toluenesulfonic acid (acid catalyst, **3**) were heated at reflux in cyclohexane, and methanol was produced as the condensate of the cyclization. The resulting dioxepin (**4**) was isolated by column chromatography and then distilled under reduced pressure prior to use, and the overall yield obtained was 21.85%. Rigorously pure monomer was required

Chemistry Department, United States Naval Academy, Annapolis, Maryland 21402, USA. E-mail: jham@usna.edu



**Scheme 1** One-step synthesis of 3-bromopropyl-functionalized dioxepin **4**.



Favored at:

- Higher temp.
- Lower concentration

Favored at:

- Lower temp.
- Higher concentration

**Scheme 2** Ring-opening metathesis polymerization (ROMP) equilibrium of monomer **4** and polymer **5**.

to avoid undesired chain transfer reactions with linear olefins (chiefly, trace amounts of **2**).

The aim was to polymerize **4** via ROMP chemistry with a suitable ruthenium metathesis catalyst (Scheme 2). To better predict and understand its ROMP behavior, the ring strain energy (RSE) of **4** was calculated as the enthalpy change ( $\Delta H$ ) for the ring-closing reaction depicted in Fig. 1A. The ring-closing metathesis reaction is isodesmic in nature, having the same number and type of bonds in the reactants and products. The RSE is therefore equal to the change in enthalpy between reactants and products (Fig. 1B), and the energy difference between reactants and products is due solely to the ring strain present in the cyclic form. Density functional theory (DFT) calculations were used to model this enthalpy change at the B3LYP/6-31G(d,p) level of theory. This method has been used to calculate RSEs in good agreement with experimentally-determined RSEs for unsubstituted cyclic olefins,<sup>38</sup> and has since been used to calculate RSEs for substituted and fused-ring cyclic olefins.<sup>38–40</sup> In comparison to other small cyclic olefins (Fig. 1C), the RSE of dioxepin **4** was substantially lower. The low RSE is partially attributable to the Thorpe-Ingold<sup>41</sup> (or “gem-dimethyl”) effect which favors the ring-closed conformation due to the steric repulsion of geminally-substituted groups, as well as the incorporated oxygen heteroatoms which impart flexibility into the small cycle, reducing the inherent ring strain.

The homopolymerization behavior of **4** was studied with respect to reaction time, catalyst type, catalyst loading, reaction temperature, and monomer concentration. The results of these experiments are detailed in Table 1. Given the low RSE of **4**,

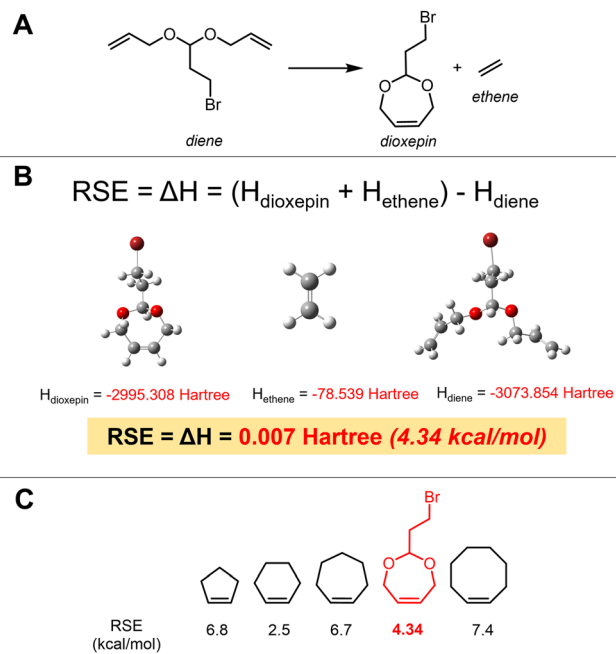


**Fig. 1** (A) Isodesmic ring-closing reaction; (B) ring strain energy (RSE) calculation of dioxepin monomer **4** (calculated enthalpy values (in red) are DFT-calculated values); (C) comparison of RSEs of **4** and other low-strain cyclic olefins commonly polymerized via ROMP (RSE literature values from ref. 38).

Grubbs' 3<sup>rd</sup> generation ruthenium catalyst (G3) was selected for its fast initiation and propagation kinetics as well as high activity at a range of temperatures.<sup>42,43</sup> Initially, the ROMP reaction of **4** was studied at ambient temperature. Two reactions (entries A & B, Table 1) were studied for the effect of reaction time with G3 as the catalyst. Entry A was allowed to proceed for 24 hours, while entry B was allowed to proceed for 4 hours. Given the small difference in reaction conversion and obtained  $M_n$  values between these two experiments, 4 hours was deemed an acceptable time period for the polymerization mixture to reach equilibrium. The remaining experiments detailed in Table 1 were each allowed to react for 4 hours. A lower activity catalyst, Grubbs' 2<sup>nd</sup> generation catalyst (G2),<sup>43</sup> exhibited little homopolymerization activity indicated by the low monomer conversion—no polymer product could be recovered for GPC analysis (Table 1, entry C). Reducing the G3 catalyst loading with respect to entry B (Table 1, entries D and E) correlated with reduced monomer conversion, though slightly higher molar mass was obtained for entry D. Elevated dispersity values throughout all studied reaction conditions suggested substantial chain transfer reactions occurred, which is commonly observed for ROMP of low RSE monomers.

Recently, it has been demonstrated that brief warm initiation of low-strain cyclic olefins (typical 5–7 membered rings) followed by propagation at low temperatures led to increased monomer conversion and living-like polymerization for some low RSE monomers (RSE values  $\sim 5$ – $7 \text{ kcal mol}^{-1}$ ), and predictable molar masses and low dispersities were obtained.<sup>44</sup> The rationale for the low temperature effect is that

Table 1 Experimental results of homopolymerization of **4**

Entry	[M]:[Cat.] <sup>a</sup>	Reaction temp. (°C)	Monomer conversion (%) <sup>b,i</sup>	Equilibrium monomer concentration (M) <sup>c</sup>	<i>M<sub>n</sub></i> (kg mol <sup>-1</sup> ) <sup>d</sup>	<i>D<sub>w</sub></i> <sup>e</sup>
A <sup>j</sup>	100 : 1	20	28.6	4.90	5.070	2.24
B	100 : 1	20	31.0	4.73	4.373	1.75
C <sup>a</sup>	100 : 1	20	3.46	6.62	— <sup>f</sup>	— <sup>f</sup>
D	250 : 1	20	14.7	5.85	6.460	2.16
E	1000 : 1	20	10.6	6.13	2.254	1.79
F	100 : 1	40/0	61.2	2.66	6.785	1.72
G	100 : 1	40/-5	63.8	2.48	7.741	2.02
H	100 : 1	40/-10	65.3	2.38	6.344	1.79
I	100 : 1	40/-15	60.7	2.70	7.017	2.02
J <sup>g</sup>	100 : 1	40/0	53.0	2.82	6.112	1.67
K <sup>h</sup>	100 : 1	40/0	21.8	5.36	3.518	1.45
L	200 : 1	40/0	51.1	4.18	7.807	1.82
M	250 : 1	40/0	50.3	3.41	6.544	1.75
N	500 : 1	40/0	28.5	4.90	9.150	1.52
O	750 : 1	40/0	20.6	5.45	5.553	1.91

<sup>a</sup> Monomer to catalyst ratio (G3 used for all experiments, except for entry C in which G2 was used). <sup>b</sup> Monomer conversion to polymer was determined by integrated the internal olefin peak (~5.82 ppm in CDCl<sub>3</sub>) with respect to the monomer olefin peak (5.72 ppm in CDCl<sub>3</sub>). <sup>c</sup> Calculated from % conversion determined by NMR, initial neat [**4**] = 6.86 M. <sup>d</sup> Number average molar mass determined from gel-permeation chromatography (GPC) calibrated with narrow dispersity polystyrene standards. <sup>e</sup> Dispersity (*M<sub>w</sub>*/*M<sub>n</sub>* where *M<sub>w</sub>* = weight average molar mass). <sup>f</sup> No polymer recovered for GPC analysis. <sup>g</sup> 50 μL dry tetrahydrofuran (THF) added to 0.5 mL neat **4**. <sup>h</sup> 100 μL dry THF added to 0.5 mL neat **4**. <sup>i</sup> Isolated yields not reported due to the small scale of the reactions and the loss of product upon workup. <sup>j</sup> Reaction time for all experiments was 4 h, except entry A (24 h).

when enthalpy of the polymerization ( $\Delta H$ ) is small and negative, lowering the temperature of the reaction reduces the influence of the  $-T\Delta S$  term on  $\Delta G$  according to the Gibbs Free Energy equation, thereby amplifying the contribution of slightly negative enthalpy on the total Gibbs Free Energy ( $\Delta G$ ) of the reaction. In a typical ROMP reaction where the cyclic olefin has a high RSE, the relief of ring strain is the primary driving force for the forward polymerization reaction (where  $\Delta G < 0$ ).

Entries F–I in Table 1 investigated the effect of initiating the polymerization in warm conditions (40 °C) for 5 minutes, then reducing the temperature for propagation. The rationale for gently warming prior to cooling the reaction mixture for the remaining duration of the reaction was that the elevated temperature helped to solubilize the catalyst in the bulk monomer and to promote efficient initiation. In past work,<sup>44</sup> 40 °C was chosen due to the boiling point of the monomer, but it is also a temperature at or below which the catalyst will reliably not degrade. Catalyst stability, catalyst solubility in the neat monomer, and efficient initiation were each a consideration in choosing 40 °C as an initiation temperature in these experiments. In this monomer/catalyst system, an appreciable enhancement in monomer conversion was observed for the variable-temperature ROMP experiments, and slightly higher molar masses were obtained. Dispersity values remained between 1.72–2.02, indicating that chain transfer reactions were still prevalent under these conditions. Notably, addition of small amounts of solvent to the polymerization mixtures (thereby lowering the monomer concentration, Table 1 entries J and K) led to lower dispersities (1.45–1.67) but also lower monomer conversions. Adjusting the monomer to catalyst ratio when initiating the polymerization at 40 °C and allowing propagation at 0 °C (Table 1, entries K–N) had the effect of

reducing monomer conversion, though the conditions for entry M achieved the highest molar mass polymer among the conditions studied.

Though there is not a significant thermodynamic driving force for the ROMP of **4**, thermodynamic barriers were overcome in this system by a combination of low temperature propagation (discussed above), the use of a high activity catalyst (G3), and maximizing monomer concentration (bulk monomer conditions). G3 exhibits a very high propagation rate constant (*k<sub>p</sub>*)<sup>43</sup> and in this system it appears that G3's high kinetic activity allowed for rapid formation of the polymer, even without a large enthalpic driving force. High monomer concentration also helped push the monomer/polymer equilibrium toward polymer product according to Le Chatelier's principle that increasing reactant concentration shifts the equilibrium towards products.

Having studied the homopolymerization behavior of **4**, attention was then turned to studying the ability of the 3-bromopropyl acetal functional group embedded in every repeat unit of **5** to undergo acid catalyzed, self-amplified degradation. Scheme 3 shows the proposed mechanism of degradation.<sup>21</sup> Upon addition of a catalytic amount of acid (H<sup>+</sup>), the acetal species is cleaved— first forming a hemiacetal intermediate, then a β-halogenated aldehyde which undergoes an elimination to form acrolein plus an equivalent of hydrobromic acid. This degradation is self-amplifying in nature because each acetal hydrolysis event generates an equivalent of acid (HBr) which can go on to catalyze the degradation of another acetal unit.

The self-amplified degradation of **4** and **5** (a sample with *M<sub>n</sub>* = 5500 g mol<sup>-1</sup>) was monitored using <sup>1</sup>H NMR spectroscopy under relatively mild acidic and buffered conditions (30 vol% pD = 5.5), as well as strongly acidic conditions (30 vol% pD = 2.2); the results of these experiments are shown graphically in



Scheme 3 Proposed mechanism of 3-bromopropyl acetal hydrolysis leading to self-amplified degradation.<sup>21</sup>

Fig. 2. The pD metric refers to the logarithmic scale measuring the concentration of  $\text{D}^+$  ions in  $\text{D}_2\text{O}$ -solvated systems, and it is analogous to the pH scale in  $\text{H}_2\text{O}$ -solvated systems. The varying pD solutions used in these studies were prepared by adding *p*-toluenesulfonic acid to  $\text{D}_2\text{O}$  (to generate acidic  $\text{D}_2\text{O}$  solutions), or a combination of sodium acetate and acetic acid (to generate a pD = 5.5 buffer in  $\text{D}_2\text{O}$  solution). For each degradation experiment in mildly acidic conditions, a 50 mM solution of 4 or 5 was prepared in a 70/30 (v/v)  $\text{DMSO-d}_6/\text{D}_2\text{O}$

mixture, where the  $\text{D}_2\text{O}$  solution was either pD = 5.5 or a pD = 5.5 acetate buffer as a control. The temperature of each reaction was maintained at 70 °C inside the NMR probe, and  $^1\text{H}$  NMR spectra were collected every 30 minutes to monitor the degradation reaction progress. To quantify the extent of degradation in the 30 vol% pD = 5.5 acidic media or the 30 vol% pD = 5.5 buffer media, the acetal proton for each sample was integrated against an internal standard to generate normalized degradation curves (Fig. 2A and B). Specifically, for 4, the disappearance of the acetal proton signal at  $\sim 4.7$  ppm (indicated with a triangle in Fig. S9 (30 vol% pD = 5.5) and Fig. S10 (30 vol% pD = 5.5 acetate buffer)) was compared to a trioxane internal standard signal at  $\sim 5.0$  ppm (indicated with a square in Fig. S9 and S10). For 5, the disappearance of the acetal proton signal at  $\sim 4.6$  ppm (indicated with a triangle in Fig. S11 (30 vol% pD = 5.5) and Fig. S12 (30 vol% pD = 5.5 acetate buffer)) was compared to a trioxane internal standard signal at  $\sim 5.0$  ppm (indicated with a square in Fig. S11 and S12). A control study was conducted to confirm no degradation of the trioxane internal standard occurred under these conditions (Fig. S13).



Fig. 2 (A)  $^1\text{H}$  NMR-monitored degradation of 4 at 70 °C in 70/30 (v/v)  $\text{DMSO-d}_6/\text{pD} = 5.5$   $\text{D}_2\text{O}$  (black circles) and 70/30 (v/v)  $\text{DMSO-d}_6/\text{pD} = 5.5$  acetate buffer in  $\text{D}_2\text{O}$  (gray triangles) (B)  $^1\text{H}$  NMR-monitored degradation of 5 at 70 °C in 70/30 (v/v)  $\text{DMSO-d}_6/\text{pD} = 5.5$   $\text{D}_2\text{O}$  (black circles) and 70/30 (v/v)  $\text{DMSO-d}_6/\text{pD} = 5.5$  acetate buffer in  $\text{D}_2\text{O}$  (gray triangles) (C) near instantaneous degradation of 5 at 70 °C in 70/30 (v/v)  $\text{DMSO-d}_6/\text{pD} = 2.2$   $\text{D}_2\text{O}$  (aqua  $^1\text{H}$  NMR spectrum is polymer 5 as-synthesized, red overlay is the  $^1\text{H}$  NMR spectrum after heating for 5 min at 70 °C, acetal proton signal denoted with an asterisk).

For 4 in the 30 vol% pD = 5.5 solution (Fig. 2A, black circles), an induction period of about 1 hour was observed, after which the acetal groups underwent accelerating degradation, consistent with mechanism shown in Scheme 3. In the presence of a 30 vol% pD = 5.5 acetate buffer, the degradation was heavily curtailed, and about 75% of the acetal units were still intact after 350 minutes (Fig. 2A, gray triangles). Similarly, 5 exhibited a short induction time of about 30 minutes (Fig. 2B, black circles), followed by precipitous self-amplified degradation consistent with the mechanism presented in Scheme 3. Presence of the 30 vol% pD = 5.5 acetate buffer limited acetal degradation to about 10% over the course of 350 minutes (Fig. 2B, gray triangles). The sigmoidal shape of the acid-amplified degradation curves of 4 and 5 is characteristic of self-amplified processes.<sup>21,45</sup> Slight differences in the degradation profiles of 4 and 5, despite being prepared at the same concentrations, may be attributable to 5 having slightly poorer solubility in the 70/30 (v/v)  $\text{DMSO-d}_6/\text{D}_2\text{O}$  solvent mixture.

Rapid degradation (on the order of minutes) of 5 was possible in 30 vol% pD = 2.2 solution at 70 °C, as shown by the complete disappearance of the acetal signal at  $\sim 4.85$  ppm (indicated with an asterisk in Fig. 2C), though hemiacetal species (a degradation intermediate) were still present in the mixture at  $t = 5$  min, evidenced by a small peak at  $\sim 4.55$  ppm

in the dark red overlay in Fig. 2C. Treatment of **5** with concentrated HCl overnight led to complete degradation of the homopolymer into small molecules, characterized by the complete disappearance of the polymer peak in GPC (Fig. S14).

Though the homopolymerization experiments of **4** did not yield high molar mass polymer, the simple and self-amplifying nature of its degradation when incorporated into macromolecules is an attractive feature to incorporate into co-polymers. Recently, interest in randomly incorporating degradable linkages into traditionally non-degradable polymers (like most polymers prepared *via* ROMP chemistry) has surged.<sup>46</sup> For example, polycyclooctene (PCO), a polymer commonly prepared *via* ROMP, is a precursor to linear high-density polyethylene (HDPE). HDPE is produced on the order of millions of tons per year, and much of what is produced ends up polluting the natural environment, where it may take centuries to degrade.<sup>47</sup> If small amounts of **4** can be incorporated into an HDPE-like co-polymer, pH gradients in the environment would allow for the co-polymer to break down into smaller segments which are more easily broken down by microbial activity.<sup>48</sup>

Scheme 4 shows how co-polymers (**7**) comprised of comonomers **4** and *cis*-cyclooctene (**6**) were prepared *via* ROMP. Experimental results of co-polymerizations between **4** and **6** are



Scheme 4 Synthesis of polyacetal/PCO co-polymers *via* ROMP.

summarized in Table 2. Initially, an experiment with a 50/50 co-monomer feed ratio was conducted at ambient temperature (Table 2, entry A) to determine whether any **4** would be incorporated into a co-polymer with **6**. <sup>1</sup>H NMR analysis of the resulting co-polymer revealed 23.47% of repeat units in the co-polymer were the degradable unit, and a unimodal GPC trace was observed for the as-synthesized co-polymer (Fig. 3, top left, solid line). Upon treatment with HCl (to degrade the embedded acetal linkages), a complex polymeric mixture was observed, and a high molar mass species which was likely pure, undegraded PCO was observed. It is possible the high molar mass species observed in the cleaved GPC traces of entries A and B in Table 2 stem from the acidic cleavage environment which may lead to cross-linking between PCO segments. A proposed mechanism for the crosslinking in acidic media is presented in Fig. S15. Slightly reducing the dioxepin feed ratio (Table 2, entry B) saw an increase in the as-synthesized molar mass, a decrease in the percent incorporation of acetal groups, but a similar post-degradation GPC trace with high molar mass species still present after acid treatment (Fig. 3, top right).

By initiating the co-polymerization at 40 °C and allowing propagation at 0 °C, similar percentages of acetal groups were incorporated into the co-polymers, and larger molar masses were obtained (Table 2, entries C and D). The difference between entries C and D in Table 2 was the catalyst loading. Acid degradation of these samples typically resulted in significant reduction of molar mass, indicating that the degradable acetal groups were more uniformly distributed throughout the co-polymers (Fig. 3, bottom). The differences in degradability between the co-polymers prepared under isothermal conditions *versus* variable temperature initiation/propagation may be attributed to more frequent cross-metathesis at higher temperatures, which seemingly resulted in less random or less uniform incorporation of the dioxepin repeat units in the co-polymer. No specific claim about the co-polymer microstructure can be made from this data alone (*i.e.* whether the co-monomer incorporation is blocky, random, alternating, *etc.*), other than co-monomers **4** and **6** appeared to co-polymerize effectively (NMR spectra of the isolated co-polymer samples are presented in Appendix 1 of the SI), and co-monomer **4** appeared to be incorporated into the growing chain repeatedly

Table 2 Results of co-polymerizations of **4** and **6**

Entry	Co-monomer feed ratio ( <b>4</b> : <b>6</b> )	Reaction temp (°C)	[M] : [cat] <sup>a,d</sup>	% <b>4</b> incorporation in co-polymer <sup>c</sup>	M <sub>n</sub> (kg/mol) <sup>b</sup>	D
A	50 : 50	25	500	23.47	10.30	2.12
Entry A, degraded					10.55	3.04
B	40 : 60	25	500	12.47	21.34	1.71
Entry B, degraded					8.31	5.17
C	50 : 50	40/0	500	17.36	18.09	1.99
Entry C, degraded					3.20	2.79
D	50 : 50	40/0	700	10.54	33.65	2.11
Entry D, degraded					6.12	4.76

<sup>a</sup> Total monomer : catalyst ratio. <sup>b</sup> Number average molar mass determined from gel-permeation chromatography (GPC) calibrated with narrow dispersity polystyrene standards. <sup>c</sup> Determined by integrating the internal allylic proton signal of polycyclooctene (~2.0 ppm) with respect to the internal allylic proton signal of polydioxepin (~4.2 ppm). <sup>d</sup> All polymerizations were catalyzed with G2, neat.



Fig. 3 GPC traces of as-synthesized polycyclooctene-co-poly(dioxepin) co-polymers (7, solid lines) and after acid treatment (dotted lines). Letter labels correspond to entries in Table 2.

between segments of PCO, supported by the fact the acid-promoted degradation resulted in a reduction in molar mass for most samples, leaving only the PCO segments behind.

While the homopolymerization of **4** is thermodynamically challenging, its co-polymerization with a moderately strained monomer (**6**) was feasible due to the enthalpic driving force contributed by **6**'s ring opening. This more favorable enthalpy from **6** appeared to effectively “pull” the polymerization of **4** along, making the overall co-polymerization thermodynamically viable. Even with a lower activity catalyst (G2), the combined thermodynamic advantage from **6**'s incorporation, alongside the apparent kinetic efficiency of the catalyst in forming cross-propagating units, enabled the successful formation of the co-polymer. Once repeat units of **4** were incorporated in the co-polymer, they were kinetically trapped within the chain, further preventing depolymerization. G2 was selected as the catalyst for the co-polymerizations reported here because a reduced propagation rate for both monomers should, in principle, reduce the relative difference in their reaction rates, allowing the less reactive monomer (**4**) a greater opportunity to be incorporated into the growing chain along-

side **6**. Similarly successful co-polymerization results between dioxepins and cyclooctadiene have been reported elsewhere.<sup>16</sup>

## Conclusion

Reported here was the one-step synthesis of a novel dioxepin monomer (**4**) amenable to homopolymerization and co-polymerization with *cis*-cyclooctene *via* ROMP. The RSE of **4** was calculated using DFT and found to be 4.34 kcal mol<sup>-1</sup>, and homopolymer **5** was prepared with  $M_n$  up to 9.15 kg mol<sup>-1</sup>. The polyacetal homopolymer exhibited a self-amplified degradation profile in acidic media due to the liberation of one equivalent of HBr with each acetal hydrolysis event. Co-polymers comprised of dioxepin monomer **4** and *cis*-cyclooctene (**6**) exhibited distribution of the acetal groups along the co-polymer backbone, so acid treatment resulted in small PCO fragments. Incorporation of **4** in small amounts may be a promising approach to imparting self-degradability into polyolefins while maintaining the desirable physical properties of the polyolefin material.

## Conflicts of interest

The authors declare no competing financial interest. The views expressed in this document are those of the authors and do not reflect the policy or position of the U.S. Naval Academy, Department of the Navy, the Department of Defense, or the U.S. Government.

## Data availability

The data supporting this article have been included as part of the SI: instrumental and experimental methods, characterization data, and supplemental GPC data and NMR spectra. See DOI: <https://doi.org/10.1039/d5py00484e>.

## Acknowledgements

The authors gratefully acknowledge support for this work from the Naval Academy Research Council, the Defense Threat Reduction Agency Service Academy Research Initiative, and the James Kinnear Summer Research Fellowship.

## References

- V. R. Feig, H. Tran and Z. Bao, Biodegradable Polymeric Materials in Degradable Electronic Devices, *ACS Cent. Sci.*, 2018, **4**, 337–348.
- S. M. McDonald, Q. Yang, Y. H. Hsu, S. P. Nikam, Z. Hu, Z. Wang, D. Asheghali, T. Yen, A. V. Dobrynin, J. A. Rogers and M. L. Becker, Resorbable barrier polymers for flexible bioelectronics, *Nat. Commun.*, 2023, **14**, 7299.
- V. Delplace and J. Nicolas, Degradable vinyl polymers for biomedical applications, *Nat. Chem.*, 2015, **7**, 771–784.
- M. A. Hillmyer and W. B. Tolman, Aliphatic polyester block polymers: Renewable, degradable, and sustainable, *Acc. Chem. Res.*, 2014, **47**, 2390–2396.
- O. Ivanchenko and M. Destarac, 1,1'-Thiocarbonyldiimidazole Radical Copolymerization for the Preparation of Degradable Vinyl Polymers, *ACS Macro Lett.*, 2024, **13**, 47–51.
- R. W. Hughes, M. E. Lott, I. S. Zastrow, J. B. Young, T. Maity and B. S. Sumerlin, Bulk Depolymerization of Methacrylate Polymers via Pendent Group Activation, *J. Am. Chem. Soc.*, 2024, **146**, 6217–6224.
- R. Whitfield, G. R. Jones, N. P. Truong, L. E. Manring and A. Anastasaki, Solvent-Free Chemical Recycling of Polymethacrylates made by ATRP and RAFT polymerization: High-Yielding Depolymerization at Low Temperatures, *Angew. Chem., Int. Ed.*, 2023, **62**, e202309116.
- J. B. Young, R. W. Hughes, A. M. Tamura, L. S. Bailey, K. A. Stewart and B. S. Sumerlin, Bulk depolymerization of poly(methyl methacrylate) via chain-end initiation for catalyst-free reversion to monomer, *Chem*, 2023, **9**, 2669–2682.
- N. E. Kamber, W. Jeong, R. M. Waymouth, R. C. Pratt, B. G. G. Lohmeijer and J. L. Hedrick, Organocatalytic Ring-Opening Polymerization, *Chem. Rev.*, 2007, **107**, 5813–5840.
- M. K. Kiesewetter, E. J. Shin, J. L. Hedrick and R. M. Waymouth, Organocatalysis: Opportunities and challenges for polymer synthesis, *Macromolecules*, 2010, **43**, 2093–2107.
- A. Tardy, J. Nicolas, D. Gigmes, C. Lefay and Y. Guillaneuf, Radical Ring-Opening Polymerization: Scope, Limitations, and Application to (Bio)Degradable Materials, *Chem. Rev.*, 2017, **117**, 1319–1406.
- M. R. Hill, T. Kubo, S. L. Goodrich, C. A. Figg and B. S. Sumerlin, Alternating Radical Ring-Opening Polymerization of Cyclic Ketene Acetals: Access to Tunable and Functional Polyester Copolymers, *Macromolecules*, 2018, **51**, 5079–5084.
- H. Sun, Y. Liang, M. P. Thompson and N. C. Gianneschi, Degradable polymers via olefin metathesis polymerization, *Prog. Polym. Sci.*, 2021, **120**, 101427.
- J. Xu and N. Hadjichristidis, Heteroatom-containing degradable polymers by ring-opening metathesis polymerization, *Prog. Polym. Sci.*, 2023, **139**, 101656.
- J. M. Fishman and L. L. Kiessling, Synthesis of functionalizable and degradable polymers by ring-opening metathesis polymerization, *Angew. Chem., Int. Ed.*, 2013, **52**, 5061–5064.
- C. Fraser, M. A. Hillmyer, E. Gutierrez and R. H. Grubbs, Degradable Cyclooctadiene/Acetal Copolymers: Versatile Precursors to 1,4-Hydroxytelechelic Polybutadiene and Hydroxytelechelic Polyethylene, *Macromolecules*, 1995, **28**, 7256–7261.
- D. Moatsou, A. Nagarkar, A. F. M. Kilbinger and R. K. O'Reilly, Degradable precision polynorbornenes via ring-opening metathesis polymerization, *J. Polym. Sci., Part A: Polym. Chem.*, 2016, **54**, 1236–1242.
- P. S. Wolfe and K. B. Wagener, An ADMET route to unsaturated polyacetals, *Macromol. Rapid Commun.*, 1998, **19**, 305–308.
- T. Debsharma, F. N. Behrendt, A. Laschewsky and H. Schlaad, Ring-Opening Metathesis Polymerization of Biomass-Derived Levoglucosenol, *Angew. Chem., Int. Ed.*, 2019, **58**, 6718–6721.
- L. Fu, X. Sui, A. E. Crolais and W. R. Gutekunst, Modular Approach to Degradable Acetal Polymers Using Cascade Enyne Metathesis Polymerization, *Angew. Chem., Int. Ed.*, 2019, **58**, 15726–15730.
- K. A. Miller, E. G. Morado, S. R. Samanta, B. A. Walker, A. Z. Nelson, S. Sen, D. T. Tran, D. J. Whitaker, R. H. Ewoldt, P. V. Braun and S. C. Zimmerman, Acid-Triggered, Acid-Generating, and Self-Amplifying Degradable Polymers, *J. Am. Chem. Soc.*, 2019, **141**, 2838–2842.
- B. R. Elling, J. K. Su and Y. Xia, Degradable Polyacetals/Ketals from Alternating Ring-Opening Metathesis Polymerization, *ACS Macro Lett.*, 2020, **9**, 180–184.
- T. Haider, O. Shyshov, O. Suraeva, I. Lieberwirth, M. Von Delius and F. R. Wurm, Long-Chain Polyorthoesters as

- Degradable Polyethylene Mimics, *Macromolecules*, 2019, **52**, 2411–2420.
- 24 P. Shieh, W. Zhang, K. E. L. Husted, S. L. Kristufek, B. Xiong, D. J. Lundberg, J. Lem, D. Veysset, K. A. Nelson, D. L. Plata and J. A. Johnson, Cleavable comonomers enable degradable, recyclable thermoset plastics, *Nature*, 2020, **583**, 542–547.
- 25 A. Mandal and A. F. M. Kilbinger, Catalytic Living ROMP: Synthesis of Degradable Star Polymers, *ACS Macro Lett.*, 2023, **12**, 1372–1378.
- 26 A. Mandal, S. Pal and A. F. M. Kilbinger, Controlled Ring Opening Metathesis Polymerization of a New Monomer: On Switching the Solvent—Water-Soluble Homopolymers to Degradable Copolymers, *Macromol. Rapid Commun.*, 2023, **44**, 1–6.
- 27 S. C. Leguizamon, K. Lyons, N. T. Monk, M. T. Hochrein, B. H. Jones and J. C. Foster, Additive Manufacturing of Degradable Materials via Ring-Opening Metathesis Polymerization (ROMP), *ACS Appl. Mater. Interfaces*, 2022, **14**, 51301–51306.
- 28 J. D. Feist, D. C. Lee and Y. Xia, A versatile approach for the synthesis of degradable polymers via controlled ring-opening metathesis copolymerization, *Nat. Chem.*, 2022, **14**, 53–58.
- 29 J. D. Feist and Y. Xia, Enol Ethers Are Effective Monomers for Ring-Opening Metathesis Polymerization: Synthesis of Degradable and Depolymerizable Poly(2,3-dihydrofuran), *J. Am. Chem. Soc.*, 2020, **142**, 1186–1189.
- 30 T. Steinbach, E. M. Alexandrino, C. Wahlen, K. Landfester and F. R. Wurm, Poly(phosphonate)s via olefin metathesis: Adjusting hydrophobicity and morphology, *Macromolecules*, 2014, **47**, 4884–4893.
- 31 H. T. Tee, I. Lieberwirth and F. R. Wurm, Aliphatic Long-Chain Polypyrophosphates as Biodegradable Polyethylene Mimics, *Macromolecules*, 2019, **52**, 1166–1172.
- 32 C. C. Chang and T. Emrick, Functional polyolefins containing disulfide and phosphoester groups: Synthesis and orthogonal degradation, *Macromolecules*, 2014, **47**, 1344–1350.
- 33 F. N. Behrendt, A. Hess, M. Lehmann, B. Schmidt and H. Schlaad, Polymerization of cystine-derived monomers, *Polym. Chem.*, 2019, **10**, 1636–1641.
- 34 T. M. McGuire, C. Pérale, R. Castaing, G. Kociok-Köhn and A. Buchard, Divergent Catalytic Strategies for the Cis/Trans Stereoselective Ring-Opening Polymerization of a Dual Cyclic Carbonate/Olefin Monomer, *J. Am. Chem. Soc.*, 2019, **141**, 13301–13305.
- 35 Y. Liang, H. Sun, W. Cao, M. P. Thompson and N. C. Gianneschi, Degradable Polyphosphoramidate via Ring-Opening Metathesis Polymerization, *ACS Macro Lett.*, 2020, **9**, 1417–1422.
- 36 B. Liu and S. Thayumanavan, Substituent Effects on the pH Sensitivity of Acetals and Ketals and Their Correlation with Encapsulation Stability in Polymeric Nanogels, *J. Am. Chem. Soc.*, 2017, **139**, 2306–2317.
- 37 H. Frauenrath and T. Philipps, A simple diastereoselective synthesis of ( $\pm$ )-eldanolide, *Tetrahedron*, 1986, **42**, 1135–1138.
- 38 A. Hejl, O. A. Scherman and R. H. Grubbs, Ring-opening metathesis polymerization of functionalized low-strain monomers with ruthenium-based catalysts, *Macromolecules*, 2005, **38**, 7214–7218.
- 39 R. Tuba, M. Al-Hashimi, H. S. Bazzi and R. H. Grubbs, One-pot synthesis of poly(vinyl alcohol) (PVA) copolymers via ruthenium catalyzed equilibrium ring-opening metathesis polymerization of hydroxyl functionalized cyclopentene, *Macromolecules*, 2014, **47**, 8190–8195.
- 40 D. Sathe, J. Zhou, H. Chen, H. W. Su, W. Xie, T. G. Hsu, B. R. Schrage, T. Smith, C. J. Ziegler and J. Wang, Olefin metathesis-based chemically recyclable polymers enabled by fused-ring monomers, *Nat. Chem.*, 2021, **13**, 743–750.
- 41 R. M. Beesley, C. K. Ingold and J. F. Thorpe, The Formation and Stability of spiro-Compounds from cyclohexane, *J. Chem. Soc., Trans.*, 1915, **107**, 1080–1106.
- 42 M. S. Sandford, J. A. Love and R. H. Grubbs, Mechanism and activity of ruthenium olefin metathesis catalysts, *J. Am. Chem. Soc.*, 2001, **123**, 6543–6554.
- 43 R. H. Grubbs and E. Khosravi, *Handbook of Metathesis, Volume 3: Polymer Synthesis*, Wiley, 2015.
- 44 W. J. Neary and J. G. Kennemur, Variable Temperature ROMP: Leveraging Low Ring Strain Thermodynamics to Achieve Well-Defined Polypentenamers, *Macromolecules*, 2017, **50**, 4935–4941.
- 45 F. Mata-Perez and J. F. Perez-Benito, The Kinetic Rate Law for Autocatalytic Reactions, *J. Chem. Educ.*, 1987, **64**, 925–927.
- 46 G. Si and C. Chen, Cyclic–acyclic monomers metathesis polymerization for the synthesis of degradable thermosets, thermoplastics and elastomers, *Nat. Synth.*, 2022, **1**, 956–966.
- 47 R. Geyer, J. R. Jambeck and K. L. Law, Production, use, and fate of all plastics ever made, *Sci. Adv.*, 2017, **3**, e1700782.
- 48 B. M. T. Gorish, W. I. Y. Abdelmula, S. Sethupathy, M. A. Dar, M. Shahnawaz and D. Zhu, Microbial degradation of polyethylene polymer: current paradigms, challenges, and future innovations, *World J. Microbiol. Biotechnol.*, 2024, **40**, 399.